Current Biology, Vol. 14, 2086–2095, December 14, 2004, ©2004 Elsevier Ltd. All rights reserved. DOI 10.1016/j.cub.2004.11.055

CLIP-170/Tubulin-Curved Oligomers Coassemble at Microtubule Ends and Promote Rescues

Isabelle Arnal,[1,*] Claire Heichette,[1] Georgios S. Diamantopoulos,[2] and Denis Chrétien[1]
[1]Equipe Structure et Dynamique des Macromolécules
Unité Mixte de Recherche 6026
Centre National de la Recherche Scientifique
Université de Rennes 1
Campus de Beaulieu
Avenue du Général Leclerc
Bâtiment 13
35042 Rennes Cedex
France
[2]Jasonpharm Société Anonyme
Ethnikis Antistaseos 26
16121 Athens
Greece

Summary

Background: CLIP-170 is a microtubule binding protein specifically located at microtubule plus ends, where it modulates their dynamic properties and their interactions with intracellular organelles. The mechanism by which CLIP-170 is targeted to microtubule ends remains unclear today, as well as its precise effect on microtubule dynamics.
Results: We used the N-terminal part of CLIP-170 (named H2), which contains the microtubule binding domains, to investigate how it modulates in vitro microtubule dynamics and structure. We found that H2 primarily promoted rescues (transitions from shrinkage to growth) of microtubules nucleated from pure tubulin and isolated centrosomes, and stimulated microtubule nucleation. Electron cryomicroscopy revealed that H2 induced the formation of tubulin rings in solution and curved oligomers at the extremities of microtubules in assembly conditions.
Conclusions: These results suggest that CLIP-170 targets specifically at microtubule plus ends by copolymerizing with tubulin and modulates microtubule nucleation, polymerization, and rescues by the same basic mechanism with tubulin oligomers as intermediates.

Introduction

Microtubules constitute a major component of the cytoskeleton in eukaryotic cells where they are essential for cell morphogenesis, intracellular trafficking and cell division. They are 25 nm tubes consisting of $\alpha-\beta$ tubulin heterodimers aligned head-to-tail along protofilaments that interact laterally to form the microtubule wall. Important for their functions are the dynamic properties of microtubules that switch stochastically between growing and shrinking states [1]. The transition from growing to shrinking is a catastrophe, and the reverse event is a rescue. This particular behavior, called dynamic instability [2], enables the rapid spatial changes of the microtubule cytoskeleton during the cell cycle. A striking example is the complete reorganization of microtubules at the onset of mitosis to form a bipolar spindle required for correct chromosome segregation [3]. Microtubules exhibit dynamic instability both in vitro and in vivo with some notable differences between the two. Microtubules assembled from pure tubulin grow slowly with very few catastrophes and rescues compared to microtubules in a cytoplasmic environment which exhibit high catastrophe and rescue frequencies despite their high growth rate. Specific proteins that modulate microtubule assembly and dynamics in cells are responsible for these differences [1, 4]: MAPs (microtubule associated proteins) stimulate tubulin polymerization whereas destabilizing factors, such as OP18/stathmin or XKCM1, increase the catastrophe frequency. The antagonist activity of these factors regulates microtubule organization in vivo. How these regulatory proteins interact with tubulin and/or microtubules is still unclear today but is important to understand to further characterize the basis of microtubule dynamics in cells.

In the last ten years, several proteins were shown to associate specifically with the growing plus end of microtubules where they control microtubule dynamics and their interaction with intracellular organelles [5–7]. Cytoplasmic linker protein CLIP-170 is the first member of this family, named +TIP (plus-end tracking protein) family, and was originally identified as a linker between endocytic carrier vesicles and microtubules [8, 9]. CLIP-170 is a homodimer with a N-terminal microtubule binding and a C-terminal organelle binding domains separated by an α-helical coil-coiled region [10, 11]. The N-terminal part contains two microtubule binding domains (the cytoskeletal associated protein-glycin-rich or CAP-GLY motifs) and localizes at microtubule plus ends in cells as does the full-length native protein [10, 12, 13]. CLIP-170 binds specifically to the growing plus end of microtubules, which led to the hypothesis that it could be also involved in microtubule dynamic regulation in addition to its organelle-targeting role [12, 13]. Consistent with this idea, the ortholog of CLIP-170 in fission yeast, Tip1p, was proposed to act as an anticatastrophe factor and guide microtubule growth toward the cell periphery [14]. Results in mammalian cells suggested a stimulation of rescues by CLIP-170 [15]. Apart from these data obtained in cells, no study was performed to determine the precise effect of CLIP-170 on microtubule dynamics in vitro. Indeed, the mechanism of the specific localization of CLIP-170 at microtubule plus end remains unclear today. It has been proposed that this protein could recognize tubulin sheets observed at microtubule growing ends, the closure of which causing its dissociation from the tube [12, 13]. Alternatively, CLIP-170 could be targeted at microtubule plus end by copolymerization with tubulin as suggested by in vitro experiments, which showed the interaction

*Correspondence: isabelle.arnal@univ-rennes1.fr

of CLIP-170 with tubulin oligomers [13]. In yeast, the binding of CLIP-170 homologs at microtubule ends requires a motor-dependent transport process [16, 17]. These various mechanisms do not exclude the involvement of other proteins, like kinases or MAPs, to regulate the affinity of CLIP-170 for tubulin and/or microtubules [18–20].

In this study, we have investigated how the N-terminal part of CLIP-170 (H2) affects microtubule assembly and dynamics in vitro. We found that H2 increased the growth rate and promoted rescues of microtubules polymerized from pure tubulin and isolated centrosomes, and stimulated microtubule nucleation. Electron cryomicroscopy revealed that H2 induced the formation of tubulin rings, the number of which decreased upon microtubule self-assembly. Interestingly, H2 also increased the proportion of outwardly curled protofilaments at microtubule ends in assembly conditions. These results suggest that CLIP-170 targets at the extremities of microtubules through copolymerization with tubulin and may also give some clues concerning how CLIP-170 is restricted to microtubule plus ends and promotes rescues.

Results

H2 Primarily Promotes Rescues

CLIP-170 has been shown to affect in vivo microtubule dynamics as a stabilizing regulating factor [14, 15]. To determine whether CLIP-170 regulates by itself microtubule dynamics or rather recruits a factor involved in this process, we analyzed the effect of the N-terminal part of CLIP-170 (named H2) on the dynamical behavior of microtubules assembled from pure tubulin. For this purpose, microtubules nucleated from centrosomes in the absence and presence of H2 were analyzed by video-enhanced DIC microscopy [21–23].

Briefly, centrosomes were preadsorbed on the surface of perfusion chambers followed by saturating the glass with a solution of pure tubulin. Samples containing increasing concentrations of tubulin (from 3.5 to 12 μM) with or without 1 μM H2 were then injected into the chamber and observed under the microscope at 37°C. The behavior of single microtubules was followed in real time and the parameters of dynamic instability were determined (Figure 1A). For microtubules assembled both with and without H2, the average growth rate increased linearly with tubulin concentration and was moderately stimulated by about 25% in the presence of 1 μM H2 compared to the control (Figures 1A and 1B). The extrapolated threshold of microtubule assembly from centrosomes decreased from 1 μM with tubulin alone to 0.5 μM with H2 (Figure 1B).

The catastrophe frequency was systematically decreased in the presence of H2 for identical tubulin concentrations (Figure 1A). However, we wondered whether this global decrease of the catastrophe frequency induced by H2 compared to tubulin alone was not simply due to the growth rate stimulation [21, 24]. To test this hypothesis, we plotted the catastrophe frequency *versus* the growth rate for the control and in the presence of 1 μM H2 (Figure 1C). The graph shows a marked decrease of the catastrophe frequency for increasing growth rates in both cases. For similar growth rates, catastrophe frequencies were identical with or without H2, suggesting that H2 had not a direct effect on catastrophes but rather indirectly decreased their frequency by increasing the growth rate. On the other hand, rescues were strongly promoted by H2 compared to the control where such events were almost nonexistent (Figures 1A and 1D). This strong effect on rescues is illustrated by comparing the life-histories of four microtubules assembled without and with H2 (Figure 1E). The tubulin concentrations (7 μM for the control and 5 μM in the presence of H2) were chosen to obtain similar values for the growth rate and the catastrophe frequency (Figure 1A).

The shrinkage rate was also affected by H2 and decreased 1.6 to 1.8 times compared to tubulin alone at the highest H2/tubulin ratios (1/3.5, 1/5, and 1/7, Figure 1A) indicating that H2 binds to the microtubule lattice. However, this inhibiting effect tended to disappear for the lowest H2/tubulin ratios (1/10 and 1/12), whereas both the growth rate and rescues were still stimulated. This result suggested that in these conditions, the effect of H2 was restricted to microtubule ends. To analyze this effect in more details, we assembled microtubules at a fixed tubulin concentration (7 μM) and increasing concentrations of H2 (Figure 1F). H2 linearly increased the growth rate up to 1.25 μM H2 (spontaneous nucleation did not allow measurements above 1.5 μM H2). In the presence of 1 and 1.25 μM H2, the shrinkage rate decreased compared to tubulin alone but, as described above, this inhibiting effect was clearly reduced for the lowest ratio of H2 *versus* tubulin (1/14). The catastrophe frequency decreased with increasing concentrations of H2 as expected by the increase in the growth rate. Finally, H2 strongly promoted rescues at each concentration used. Altogether, these results show clearly that H2 modulates directly microtubule dynamics, essentially by promoting rescues, and thus, does not require other factors to induce this effect.

H2 Stimulates Microtubule Spontaneous Nucleation

The video-microscope analysis revealed that high concentrations of H2 stimulated microtubule spontaneous nucleation. Although this stimulation might not be relevant to the in vivo situation, we wondered if it could give us insight into the molecular mechanisms involved in the effect of H2 on microtubule dynamics.

One classical method used to analyze microtubule nucleation is to determine the critical tubulin concentration for self-assembly by following the changes in absorbance at 350 nm by spectrophotometry [25]. For tubulin alone, we found a critical concentration of 21 μM (Figure 2A). We could not determine a precise critical tubulin concentration in the presence of H2 due to the formation of microtubule bundles that abnormally increased the turbidity during microtubule polymerization. However, electron cryomicroscopy observation of microtubules assembled with 2.5 μM tubulin in the presence of 1 μM H2 (Figure 2B) showed that H2 reduced at least 8 times the critical tubulin concentration (down to 2.5 μM compared to 21 μM with tubulin alone).

A

Tubulin (μM)	3.5	5		7		10		12	
H2 1 μM	+*	-	+	-	+	-	+	-	+
H2/Tubulin	1/3.5		1/5		1/7		1/10		1/12
Vg (μm/min)	0.59 (0.30) n=265	0.61 (0.35) n=701	0.79 (0.38) n=682	0.88 (0.41) n=574	1.12 (0.46) n=441	1.31 (0.42) n=544	1.75 (0.56) n=694	1.67 (0.43) n=386	2.10 (0.70) n=501
Vs (μm/min)	12.5 (4.4) n=78	20.0 (6.1) n=104	13.6 (6.3) n=140	22.5 (8.0) n=75	12.3 (4.3) n=109	26.8 (11.5) n=65	17.2 (11.0) n=40	25.9 (16.6) n=12	25.4 (11.3) n=44
F_{cat} (events/min)	0.281 n=28	0.195 n=26	0.158 n=23	0.168 n=21	0.127 n=18	0.072 n=10	0.039 n=6	0.035 n=4	0.026 n=4
Fres (events/min)	0.34 n=2	0 -	0.44 n=7	0 -	0.60 n=7	0.16 n=1	0.99 n=6	0 -	1.26 n=3
Time (min)	84	139	161	131	152	129	158	112	154

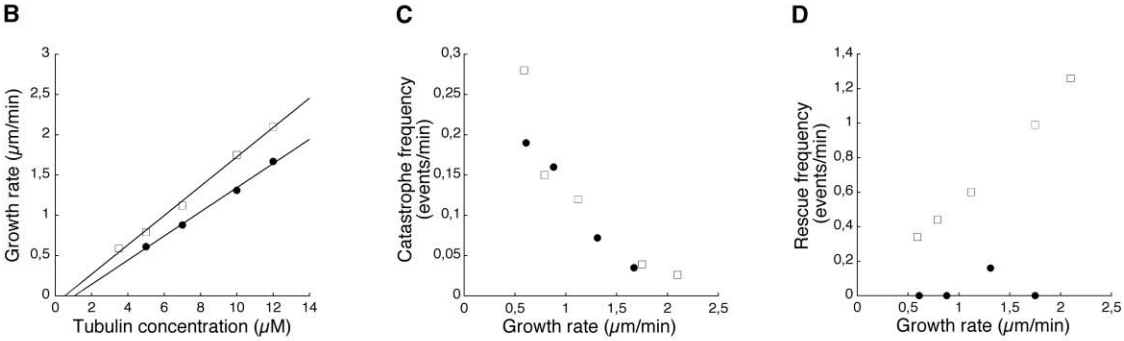

E

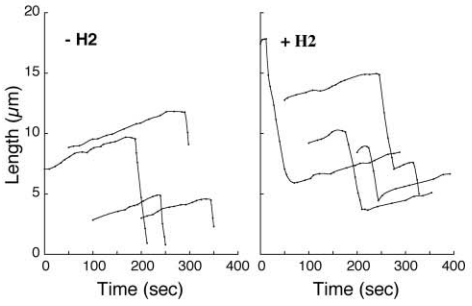

F

H2 (μM)	0	0.5	1	1.25
H2/Tubulin		1/14	1/7	1/5.6
Vg (μm/min)	0.88 (0.41) n=574	0.95 (0.47) n=576	1.12 (0.46) n=441	1.16 (0.56) n=440
Vs (μm/min)	22.5 (8.0) n=75	18.5 (8.6) n=164	12.3 (4.3) n=109	13.7 (5.9) n=125
F_{cat} (events/min)	0.168 n=21	0.142 n=32	0.127 n=18	0.081 n=13
Fres (events/min)	0 -	0.56 n=10	0.60 n=7	0.65 n=14
Time (min)	131	239	152	180

Figure 1. H2 Promotes Rescues

(A) Dynamical parameters of microtubules polymerized from centrosomes at increasing concentrations of tubulin with or without 1 μM H2. Standard deviations are given in parentheses and "n" indicates the number of total events measured. The "time" represents the total time of recording and analysis. *Microtubule dynamics were not recorded with 3.5 μM tubulin alone because microtubules were too short to be measured. V_g, growth rate; V_s, shrinkage rate; F_{cat}, catastrophe frequency. F_{res}, rescue frequency. (B) Microtubule growth rate versus tubulin concentration in the absence (●) and in the presence (□) of 1 μM H2. Linear regression was performed on the two complete data sets. (C) Catastrophe frequency versus growth rate in the absence (●) and in the presence (□) of H2. (D) Rescue frequency versus growth rate in the absence (●) and in the presence (□) of H2. (E) Life-history traces of microtubules assembled at 7 μM tubulin (left) and 5 μM tubulin in the presence of 1 μM H2 (right). (F) Dynamical parameters of microtubules polymerized at 7 μM tubulin and increasing concentrations of H2.

To further characterize the effect of H2 on microtubule self-assembly, 50 μM tubulin was polymerized in the absence and in the presence of 0.16 μM H2 and the length and total quantity of microtubules were determined by negative staining electron microscopy during the assembly phase (arrows in Figure 2C, see Experimental Procedures for details). The low concentration of H2 (0.16 μM) was chosen to minimize as much as possible the formation of microtubule bundles. After 6 min of assembly, the total number of microtubules was 1.6 to 2 times higher in the presence of H2 compared to the control, and with a length distribution shifted down toward short microtubules (average length of 16 μm with H2 compared to 26 μm without H2, Figure 2D). These

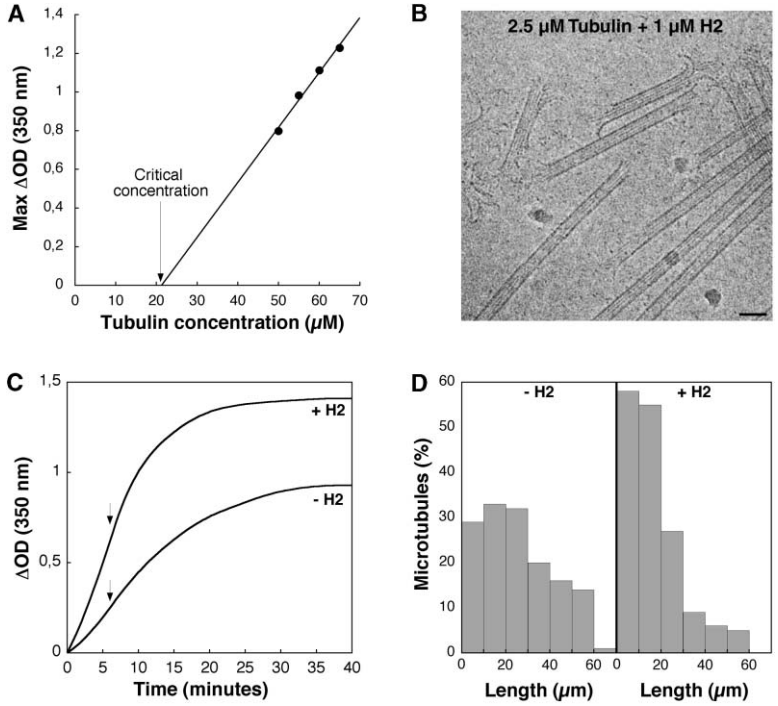

Figure 2. H2 Increases Spontaneous Microtubule Nucleation

(A) Determination of the critical tubulin concentration for microtubule self-assembly. Increasing concentrations of pure tubulin was polymerized at 37°C and the maximum values of OD obtained at the plateau were plotted against tubulin concentration (see Experimental Procedures for more details). The critical concentration is given by the intersection between the linear regression curve and the *x* axis. (B) Vitreous ice embedded microtubules polymerized with 2.5 μM tubulin and 1 μM H2 after 1 min of assembly at 37°C. (C) 50 μM tubulin was polymerized in the absence and in the presence of 0.16 μM H2. Samples were fixed during the elongation phase after 6 min of assembly (black arrows) before being ultracentrifuged and negatively stained for electron microscopy (see Experimental Procedures). (D) Distributions of microtubule lengths in the absence and in the presence of H2. OD, optical density. The scale bar represents 50 nm.

results show clearly that H2 stimulates microtubule nucleation, and thus, may interact with tubulin in solution in order to form prenuclei competent for microtubule assembly.

H2 Induces the Formation of Curved Tubulin Oligomers in Solution and at Microtubule Ends

The previous analysis revealed that H2 modulates microtubule assembly and dynamics by stimulating nucleation, increasing the growth rate and promoting rescues. To investigate the mechanisms underlying these effects, we used electron cryomicroscopy to analyze the structures involved in these processes. By contrast with the video-light microscope analysis, we chose self-assembly conditions where all the microtubules are in the growing state during the initial elongation phase.

Previous studies have shown that H2 promotes tubulin oligomerization at 4°C [13]. In order to characterize the H2/tubulin complexes, tubulin (50 μM) with or without H2 (4 μM) was incubated with 1 mM GTP at 4°C to prevent microtubule assembly (Figure 3A). Addition of H2 resulted in the apparition of curved tubulin oligomers, rings (mostly single with some double) and spirals that were not observed with tubulin alone (Figure 3B). The average radius of single rings was 19.1 ± 1.8 nm and the inner and outer radii of double rings were 16 ± 1.8 nm and 22.5 ± 3.0 nm respectively, values similar to those observed previously with GDP-tubulin [26–29]. We thus wondered whether H2 imposed this curved conformation to the GTP-tubulin present in solution. Short curved tubulin oligomers could already be observed with pure tubulin at 50 μM (arrow in Figure 3B). In addition, when the tubulin concentration was adjusted to 140 μM, the proportion of curved oligomers increased and a few rings with a radius of 17.6 ± 1.9 nm, similar to that of the H2-tubulin induced rings, started to appear (Figure 3C). These observations suggest that tubulin in solution has an intrinsically curved conformation and that H2 only crosslinks tubulin dimers.

We then wondered whether these rings were involved in microtubule assembly. Microtubules were polymerized at 50 μM tubulin in the presence of increasing concentrations of H2 (0.16 to 4 μM, Figure 4). Samples were frozen in the elongation phase after 6 min in the control and in the presence of 0.16 μM H2, and after 15 s in the presence of 4 μM H2. With tubulin alone, the microtubule extremities were mostly blunt and the background did not reveal any particular structures (Figure 4A). However, in the presence of 0.16 μM H2 (Figure 4B), curved oligomers with a radius of curvature similar to that of rings present in solution were observed at microtubule ends (Figure 4B, inset). Increasing the H2 concentration up to 4 μM resulted in the appearance of short microtubules and sheets with rings frequently associated with their ends (Figure 4C, arrowhead). To analyze in more details the structure of microtubule ends in these different assembly conditions, we classified them into four main categories: blunt ends (Figure 4D), curled ends (Figure 4E), sheets (Figure 4F) and sheets with outwardly curled protofilaments (called "curled sheets", Figure 4G). Two-dimensional sheets of tubulin are typical of growing microtubules whereas curled ends are usually observed in disassembly conditions [23, 30–33]. Microtubules assembled with 50 μM tubulin presented mostly blunt ends (81.1%) (Figure 4H). With 0.16 μM H2, the proportion of curled ends increased to 39%, while at 4 μM H2, the majority of the structures observed were sheets, with (14.8%) or without (42.1%) curled extremities. A proportion of 33% of these sheets were free in solution (whereas no free sheets were observed in the control).

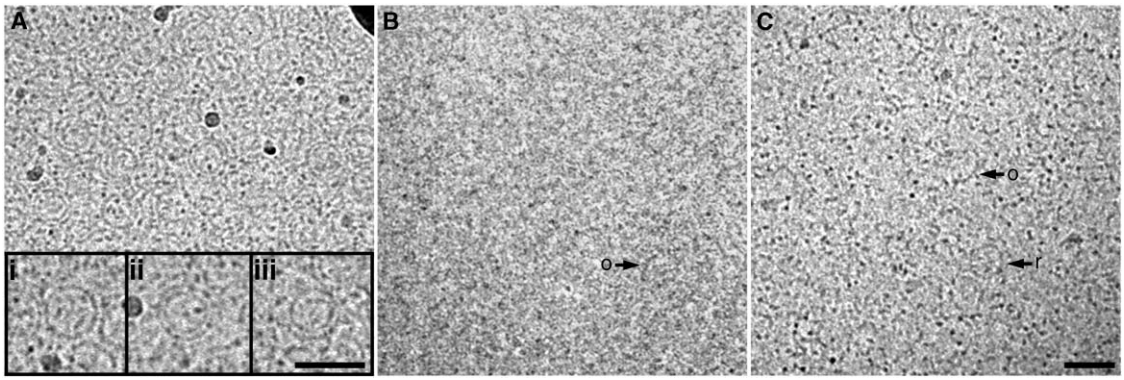

Figure 3. H2 Promotes Tubulin Ring Formation at 4°C

50 μM tubulin was incubated with 1 mM GTP at 4°C in the presence (A) and in the absence (B) of 4 μM H2 and observed by electron cryomicroscopy. (i) Single rings. (ii) Double rings. (iii) Spirals. Curved oligomers and a few rings could be visualized with tubulin alone and GTP by increasing the tubulin concentration up to 140 μM (C). o, curved oligomer; r, ring. The scale bar represents 50 nm.

The high proportion of curled oligomers at microtubule ends in the presence of H2, and the fact that their radius of curvature was similar to that of the H2-tubulin rings observed at 4°C (Figure 3A), suggested that rings could be involved in the process of microtubule assembly. To test this hypothesis, we asked whether rings tended to disappear during the assembly of microtubules. A low tubulin concentration (2.5 μM tubulin in the presence of 1 μM H2) was chosen to reduce the density of microtubules and facilitate the counting of rings compared to the previous conditions. Samples were frozen and analyzed by electron cryomicroscopy by taking images at random without a preselection of the density of rings present in the background (see Experimental Procedures for details). Since the number of rings and microtubules were variable inside a same specimen depending on the areas that were imaged, the negatives were classified according to their ring density (Figure 5A: 0 rings, B: 1-100 rings, C: above 100 rings). The histogram in Figure 5D shows the ring density distributions in specimens taken after 1 and 25 min of assembly. After 1 min, the background was clearly dominated by rings while after 25 min, it was relatively clean with a vast majority of images showing no rings. In addition, the analysis of microtubule end structures in these conditions showed a low proportion of blunt ends (10.1%) and a high proportion of curled ends (30%) and sheets with or without curled extremities (59.9%) after 1 min of assembly (Figure 5E). After 25 min of assembly, the proportion of sheets decreased to 38.5% and blunt ends increased to 26.5%. It should be noted that 51% of the sheets observed at the beginning of assembly were free in solution whereas this proportion decreased to 24% after 25 min of assembly. Altogether, these results indicate that the tubulin rings observed in the presence of H2 are not a storage form of tubulin but may be directly involved in the assembly process.

Discussion

The localization of CLIP-170 at microtubule plus ends remains unclear today and has been proposed to involve different mechanisms such as recognition of microtubule end structure, copolymerization with tubulin and/or interaction with other MAPs [12, 13, 16–20]. In addition, a direct effect of CLIP-170 on microtubule dynamics has been suggested by different studies [14, 15] but has never been demonstrated in vitro. In this study, we have asked whether the N-terminal part of CLIP-170 (H2) could modulate the dynamic properties of microtubules assembled from pure tubulin in the absence and presence of centrosomes, and if so, what were the structural mechanisms involved. We found that CLIP-170 primarily promoted rescues and stimulated microtubule self-assembly. Electron cryomicroscopy revealed that H2 induced the formation of curved tubulin oligomers and rings in solution. Curved oligomers were also found at the extremity of growing microtubules, a mechanism consistent with the targeting of H2 at microtubule ends by copolymerization with tubulin. Based on these observations, we propose a structural model that may account for the H2 rescue-promoting activity and its confinement at microtubule ends.

H2 Promotes Rescues and Stimulates Microtubule Self-Assembly

The video-microscope analysis revealed that the main effect of H2 was to promote rescues of microtubules nucleated by isolated centrosomes (Figure 1), which is consistent with the rescue-promoting activity of CLIP-170 in mammalian cells [15]. Our results also demonstrated that H2 directly modulated microtubule dynamics without the need of intermediate factors. The decrease in the catastrophe frequency that we observed in the presence of H2 was a direct consequence of the increase in the microtubule growth rate. In addition, the shrinkage rate was reduced for H2/tubulin ratios above 1/10, indicating that in these conditions, H2 bound to the microtubule lattice and reinforced the lateral interactions between protofilaments. Interestingly, at lower H2/tubulin ratios, the shrinkage rate was not affected anymore while both the growth rate and rescues were still stimulated, suggesting that H2 has a higher affinity for microtubule ends than for the microtubule lattice. In agreement with this result, CLIP-170 has been shown to bind all the length of microtubules when overex-

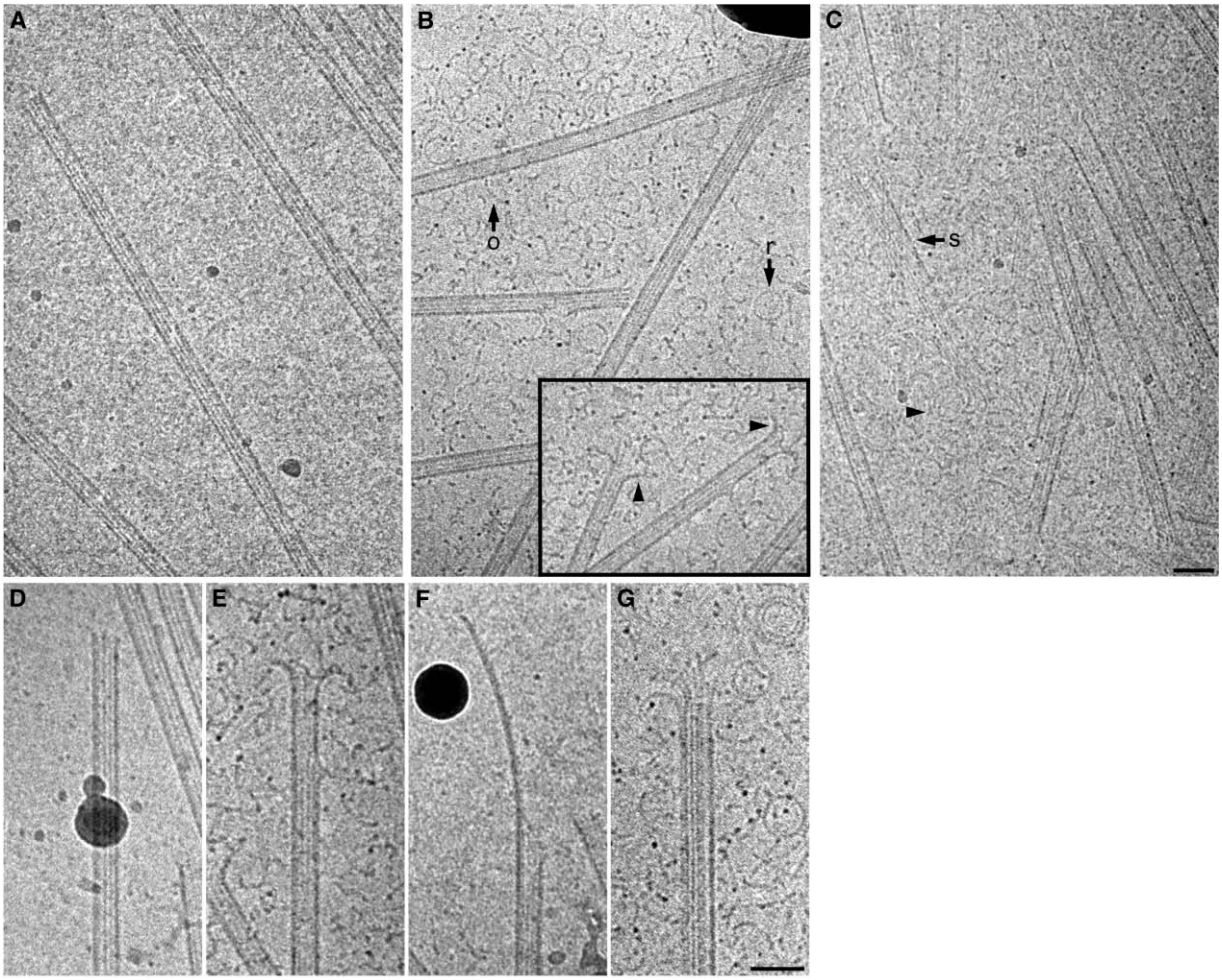

H

	50 μM Tubulin	50 μM Tubulin + 0.16 μM H2	50 μM Tubulin + 4 μM H2
Blunt	81.1 % (56)	40.2 % (33)	21 % (20)
Curled	11.6 % (8)	39 % (32)	22.1 % (21)
Sheet	7.3 % (5)	11 % (9)	42.1 % (40)
Curled sheet	-	9.8 % (8)	14.8 % (14)

Figure 4. H2 Induces the Formation of Curved Tubulin Oligomers at Microtubule Ends

(A) Vitreous ice embedded microtubules polymerized in the presence of 50 μM tubulin after 6 min of assembly at 37°C. (B) Vitreous ice embedded microtubules polymerized in the presence of 50 μM tubulin and 0.16 μM H2 after 6 min of assembly at 37°C. (C) Vitreous ice embedded microtubules polymerized in the presence of 50 μM tubulin and 4 μM H2 after 15 s of assembly at 37°C. (D) Blunt end. (E) Curled end. (F) Side view of a two-dimensional sheet of tubulin. (G) Front view of a sheet with outwardly curled protofilaments ("curled sheet"). (H) Quantification of microtubule end structures in the presence of increasing concentrations of H2. The number of ends examined is indicated in parentheses. Arrowheads indicate curved oligomers and open rings located at sheet and microtubule ends. o, curved oligomer ; r, ring ; s, sheet. The scale bar represents 50 nm.

pressed in cells [10]. Self-assembly was observed at high H2/tubulin ratios showing that H2 had also an effect on microtubule nucleation. Indeed, microtubule self-assembly could be obtained at a tubulin concentration as low as 2.5 μM in the presence of 1 μM H2 whereas the critical concentration for microtubule self-assembly was 21 μM (Figure 2). This effect of H2 on microtubule spontaneous nucleation is probably not relevant in vivo. However, H2 could act on nucleation from centrosomes in cells, as suggested by the video-microscope analysis

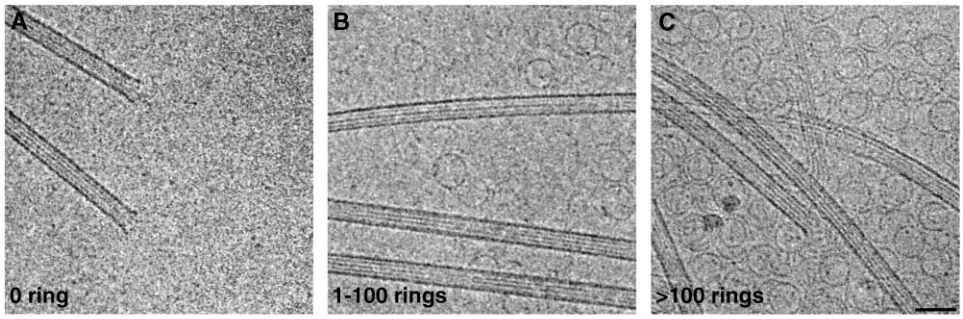

D

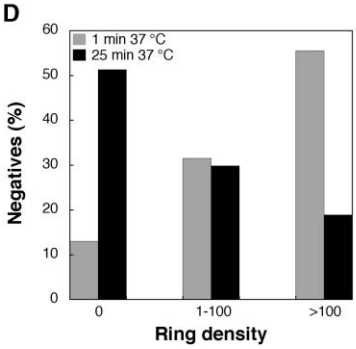

E

	1 minute	25 minutes
Blunt	10.1 % (81)	26.5 % (186)
Curled	30 % (240)	35 % (247)
Sheet	49 % (392)	32.3 % (227)
Curled sheet	10.9 % (87)	6.2 % (43)

Figure 5. The Proportion of H2-Induced Tubulin Rings Decreases during Microtubule Assembly

Microtubules were polymerized in the presence of 2.5 μM tubulin and 1 μM H2. Samples were frozen after 1 min and 25 min of incubation at 37°C and observed by electron cryomicroscopy. Negatives were classified in three different groups depending on their ring density: 0 ring (a typical area is presented in A), 1 to 100 rings (B), more than 100 rings per negative (C). (D) Ring density distributions after 1 min (in gray) and 25 min (in black) of assembly. Results include a total of 38 negatives at 1 min and 37 negatives at 25 min. (E) Quantification of microtubule end structures. The number of ends examined is indicated in parentheses. The scale bar represents 50 nm

(Figure 1B). Further studies will be needed to explore this effect in more details.

H2 Promotes Tubulin-Curved Oligomers Formation in Solution and at Microtubule Ends: Consequences for Microtubule Assembly Mechanisms

We used electron cryomicroscopy to investigate the structural basis of the effects of H2 on microtubule dynamics. Analysis of the H2-tubulin solution at 4°C revealed the presence of curved oligomers and rings (Figure 3A) whose diameters were similar to those observed previously with GDP-tubulin [26–29]. Whether this curved conformation is imposed by H2 or is intrinsic to GTP-tubulin in solution is unclear. Some curved oligomers and rings with similar radii could be observed with tubulin alone in the presence of GTP (Figure 3B and C) but these may reflect a basal GTP-hydrolysis activity of tubulin at 4°C. We next wondered whether these rings were involved in microtubule assembly in the presence of H2. Analysis of microtubules during the assembly phase showed that curved oligomers with a radius of curvature similar to that of rings observed in solution were present at their ends (Figures 2B, 4B, and 4C). In addition, we found that the number of rings decreased as microtubule polymerized (Figure 5), suggesting that they were involved in this process. Whether rings bind directly to microtubule ends and subsequently unroll, or first dissociate into dimers/oligomers before assembly [34], remains to be investigated. An alternative pathway is that H2 interacts with the microtubule lattice, especially at high ratios of H2 versus tubulin, for which the shrinkage rate inhibition indicates such an interaction along the microtubule wall. H2 would then modulate microtubule dynamics through a lattice-based effect near the microtubule ends by longitudinally crosslinking incoming tubulin dimers/oligomers and/or by reinforcing their lattice lateral interactions, as proposed for other MAPs [35].

To account for the effects of H2 on microtubule nucleation, polymerization and rescue, we propose a model that involves H2-tubulin rings and/or curved oligomers as intermediates. Microtubule self-assembly is energetically limited by the nucleation step that should involve the formation of tubulin oligomers constituting the starting point of sheets in pure tubulin solutions [36, 37]. In this regards, the H2-tubulin oligomers could act as preformed protofilaments and favor the first steps of nucleation. Microtubule polymerization would then occur by the addition of H2-tubulin oligomers at microtubule ends (Figure 6A), as suggested by the high proportion of curled extremities observed during self-assembly. A stronger affinity of the incoming H2-tubulin oligomers for the microtubule lattice compared to tubulin alone would explain the stimulating effect of H2 on the polymerization rate. Along the same line, the formation of complexes between tubulin and several different MAPs has already been proposed to explain their stimulating effect on microtubule polymerization [24, 38, 39]. It should be also noted that original studies on the polymerization of microtubule proteins (tubulin

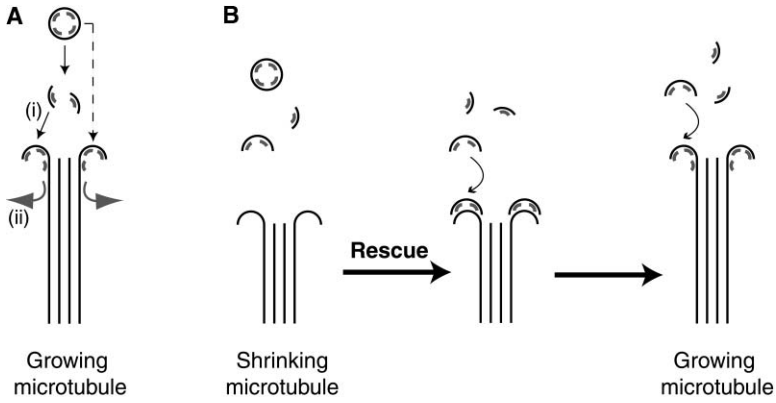

Figure 6. Models for H2-Targeting and Rescue-Promoting Activity

(A) Mechanism of targeting. H2 (in gray) longitudinally crosslinks tubulin dimers, inducing the formation of rings which might be intermediates of microtubule assembly, either directly (dashed arrow) or after their dissociation into shorter oligomers (plain arrow). H2 binds likely inside rings, since this surface is exposed after incorporation in the microtubule wall [29], with a stochiometry of 1 H2 to 4.3 tubulin dimers [11]. A consequence of this assembly mechanism is that H2 targets at microtubule ends through copolymerization with tubulin (i). The "curved-to-straight" structural change occurring during the microtubule wall formation would induce the release of H2 and confine it to the growing end (ii). (B) Mechanism of rescue. During shrinking events, microtubule ends display outwardly curled protofilaments with exposed free lateral bonds that could interact with H2-tubulin oligomers. The subsequent reinforcement of the lateral interactions between protofilaments would lead to a rescue characterized by a recovery of polymerization.

plus MAPs) proposed tubulin rings and/or curved oligomers as assembly intermediates [26, 40, 41], in agreement with our observations with H2. Concerning rescues, the individual curled protofilaments peeling out from depolymerizing microtubule ends [23, 30–33] may represent exposed sites that can interact laterally with H2-tubulin oligomers, especially if H2 reinforces the tubulin lateral interactions (Figure 6B). The subsequent straightening of protofilaments would initiate a new round of polymerization. Thus, the same mechanism with tubulin rings/oligomers as intermediates would explain the stimulating effect of H2 on nucleation, polymerization and rescues.

H2 Targets at Microtubule Ends by Copolymerizing with Tubulin

The presence of curved oligomers at the extremities of growing microtubules strongly suggests that H2 specifically targets to their ends by copolymerizing with tubulin (Figure 6A, (i)). Such a mechanism was already hypothesized by in vitro studies showing the oligomerization of tubulin in the presence of H2 [13]. An important question is to understand how CLIP-170 is restricted to microtubule ends in vivo [12, 13]. The video-microscope analysis revealed that at the lowest H2/tubulin ratios, the effect of H2 was restricted to microtubule ends where curved oligomers were present, as demonstrated by electron cryomicroscopy. We thus speculate that H2 may have a higher affinity for the "curved" conformation of tubulin compared to the "straight" one present in the microtubule wall (Figure 6A (ii)). Upon assembly, the "curved-to-straight" conformational change induced by the closure of the microtubule wall would decrease the affinity of H2 for tubulin and explain its release from the microtubule lattice. Considering such a higher affinity of H2 for curved tubulin, we cannot exclude that its targeting mechanism may involve a direct recognition of sheets at microtubule growing ends and curled extremities of depolymerizing microtubules. To test this model, it will be necessary to determine precisely the relative affinities of H2 for tubulin in rings and microtubules. Of course, this mechanism may be regulated in vivo by other factors such as phosphorylation, interaction with other MAPs/+TIPs, or active transport by motor proteins [16–20].

Implications for the In Vivo Function of CLIP-170

It is well established that CLIP-170 is involved in the control of microtubule dynamics in vivo, either by inhibiting catastrophes in yeasts [14] or promoting rescues in mammalian cells [15]. Our results clearly demonstrate that CLIP-170 modulates directly microtubule dynamics and is a rescue factor. In cells, CLIP-170 could increase tubulin polymerization at microtubule plus ends by enhancing both tubulin dimer addition and rescue events. Depending on the subcellular localization of CLIP-170, this would lead to a preferential guidance of microtubules toward specific cell structures where they would be captured and transiently stabilized [5–7]. Other members of the +TIP family affect microtubule dynamics, in particular the human EB1 protein that was shown to stabilize microtubules in *Xenopus* egg extracts by increasing rescues and decreasing catastrophes [42]. The authors favored a direct recognition of microtubule ends by EB1 where it would stabilize protofilament extensions. Such a mechanism could involve a higher binding affinity of EB1 for the curved shape of tubulin observed at microtubule ends, as we described for CLIP-170. Further studies of the in vitro effect of +TIPs on microtubule dynamics and structure will be necessary to understand clearly the different mechanisms underlying their functions.

Experimental Procedures

Protein Purification

Tubulin was purified from pig brains by two cycles of assembly/disassembly followed by a phosphocellulose chromatography and was cycled once more to remove free nucleotides [43]. Tubulin with GDP bound to its E-site was stored in BRB80 buffer (80 mM Pipes, 1 mM $MgCl_2$ and 1 mM EGTA, pH 6.8) at –80°C. The H2 fragment corresponds to the dimeric N-terminal part of CLIP-170: a head domain of 350 amino acids (which contains the two microtubule binding sites) and a short coil-coiled region of 131 amino acids allowing dimerization [11]. Recombinant H2 with a 6-histidine tag was purified from *Escherichia coli* following the protocol from Scheel et al. [11]. After the elution of H2 from the metal affinity column, proteins were concentrated, dialyzed against BRB80 buffer and

stored at –80°C. All protein concentrations were measured using a Bradford assay with Bovine Serum Albumin as a standard.

Video-Microscopy and Data Analysis

Samples were prepared in perfusion chambers made of a slide and a coverslip separated by two strips of double-sided tape [35]. Centrosomes purified from KE-37 lymphoblastic human cells [44, 45] were first perfused into the chamber on ice at a final concentration of 1.8×10^7 centrosomes/ml. The surface of the perfusion chamber was saturated by flowing a large volume of pure tubulin. The mixture containing tubulin with 1 mM GTP in the absence or in the presence of H2 was incubated 10 min at 4°C before being perfused in the chamber and microtubule assembly was observed under an Olympus BX51 microscope with its stage, objective and condenser heated to 37°C. The microscope was equipped with DIC (Differential Interference Contrast) prisms, an Apochromat 60×/1.4 NA oil immersion objective, an 8-bit black and white video camera (Sony, XC-ST70/CE) and an Argus 20 image processor (Hamamatsu). Images were recorded every 2 s for periods of about 5 min on a PC using Simple PCI software from Hamamatsu. Microtubule dynamics measurements and data analysis were performed using NIH-Image and Kaleidagraph softwares as described before [23]. Differences between experiments with and without H2 were evaluated by a t test with a confidence level of 95%.

Microtubule Self-Assembly and Determination of the Critical Tubulin Concentration

Tubulin concentration was adjusted to 50 μM in BRB80 in the presence of 1 mM GTP. After 10 min of incubation at 4°C, microtubule assembly was induced by shifting the temperature at 37°C and monitored turbidimetrically at 350 nm in a UVIKON spectrophotometer. To test the effect of H2, increasing concentrations of the purified fragment were added to the tubulin mixture and incubated 10 min on ice before polymerization. To calculate the critical tubulin concentration needed for self-assembly, microtubule polymerization was carried out at increasing tubulin concentrations (50, 55, 60 and 65 μM) and followed at 350 nm as described above. The maximum optical densities reached at the plateau, reflecting the total amount of microtubules polymerized, were plotted against the tubulin concentrations. The critical concentration (21 μM) was given by the intersection of the linear regression curve with the *x* axis.

Determination of Microtubule Length and Quantity by Negative-Staining Electron Microscopy

Microtubules were assembled at 37°C with 50 μM tubulin in the absence and in the presence of 0.16 μM H2, and were fixed in the elongation phase by diluting the samples in warmed BRB80 buffer containing 0.2% glutaraldehyde. 150 μl of the resulting suspensions were transferred into Beckman centrifuge tubes (5 × 41 mm) containing a small plexiglass insert at the bottom to support the carbon coated electron microscope grid [45]. Tubes were then introduced in a TLS55 Beckman rotor and ultracentrifuged at room temperature during 90 min at 250 000 g. Grids were picked up and negatively stained by applying 4 μl of a 1% uranyl acetate solution over a period of 30 s before blotting. Microtubules were observed on a FEI Technai 20 electron microscope equipped with a cooled CCD 2K camera (GATAN). Images were recorded at a final magnification of 330× using the Digital Micrograph software (GATAN). A total of 145 microtubules for the control and 160 in the presence of H2 were directly measured on the screen. The number of microtubules of the initial solutions was determined as described previously [45]. In the presence of H2, we had to take into account the bundles. For that, we estimated the proportion of bundles to 6% (compared to the total number of counted microtubules) with a minimum of 5 and a maximum of 10 microtubules per bundle. The minimum and maximum number of microtubules included in the bundles could then be calculated and added to the number of isolated microtubules to estimate the total number of polymers.

Specimen Preparation and Electron Cryomicroscopy

Vitreous-ice embedded samples were prepared as previously reported [46]. Briefly, 4 μl of the solution were applied onto a holey carbon grid maintained in a humid atmosphere at 37°C [23]. After 15 s to 6 min of assembly depending on the condition used (see results), the droplet was blotted and plunged quickly into liquid ethane. Specimens were stored in liquid nitrogen and observed in a Philips CM 12 electron microscope using a Gatan stage precooled with liquid nitrogen. Images were recorded on Kodak SO 163 films under low dose conditions and about 2.5 μm of underfocus. For the analysis of the density of rings, the areas to be imaged were chosen at low magnification with the only criteria that the ice thickness was thin enough to be recorded on the negative. The images were thus taken "blind" without a preselection of the density of rings present in the background.

Image Analysis

Negatives were digitized with an Epson scanner at 1200 dpi. The radius of tubulin rings was measured using the NIH-Image Software. For microtubule end structure analysis, we used Adobe Photoshop software. The extremities were classed into four different categories: blunt ends, curled ends, sheets and sheets with outwardly curved protofilaments (called "curled sheets"). The percentage of each type of microtubule ends was calculated with respect to the total number of extremities that we could identify. In the presence of high concentration of H2, a lot of extremities could not be classified because of the high background of rings and free sheets in solution. To determine the density of rings, these were counted directly on the digitized negatives. For high densities, an average number was estimated by counting the rings on small areas of 1 squared centimeter each and extrapolated to the entire surface of the negative. Only clearly identified rings were taken into account in the calculations. The curvature of oligomers observed at microtubule ends was determined using the NIH-Image software by overlapping a circle on the curved extremity and measuring its radius.

Acknowledgments

We would like to thank Dr. A.A Hyman, Dr. F. Perez, Dr. D. Thomas, and Dr. O. Valiron for their helpful comments on the manuscript. We also thank Fabrice Senger for productive discussion. This work was supported by grants from the Ligue Contre le Cancer, the Association pour la Recherche sur le Cancer, and Rennes Métropole.

Received: May 24, 2004
Revised: October 14, 2004
Accepted: October 15, 2004
Published: December 14, 2004

References

1. Desai, A., and Mitchison, T.J. (1997). Microtubule polymerization dynamics. Annu. Rev. Cell Dev. Biol. *13*, 83–117.
2. Mitchison, T., and Kirschner, M. (1984). Dynamic instability of microtubule growth. Nature *312*, 237–242.
3. Hyman, A.A., and Karsenti, E. (1996). Morphogenetic properties of microtubules and mitotic spindle assembly. Cell *84*, 401–410 (1996).
4. Kinoshita, K., Habermann, B., and Hyman, A.A. (2002). XMAP215: A key component of the dynamic microtubule cytoskeleton. Trends Cell Biol. *12*, 267–273.
5. Carvalho, P., Tirnauer, J.S., and Pellman, D. (2003). Surfing on microtubule ends. Trends Cell Biol. *13*, 229–237.
6. Galjart, N., and Perez, F. (2003). A plus-end raft to control microtubule dynamics and function. Curr. Opin. Cell Biol., 48–53.
7. Howard, J., and Hyman, A.A. (2003). Dynamics and mechanics of the microtubule plus end. Nature *422*, 753–758.
8. Rickard, J.E., and Kreis, T.E. (1990). Identification of a novel nucleotide-sensitive microtubule-binding protein in HeLa cells. J. Cell Biol. *110*, 1623–1633.
9. Pierre, P., Scheel, J., Rickard, J.E., and Kreis, T.E. (1992). CLIP-170 links endocytic vesicles to microtubules. Cell *7*, 887–900.
10. Pierre, P., Pepperkok, R., and Kreis, T.E. (1994). Molecular characterization of two functional domains of CLIP-170 in vivo. J. Cell Sci. *107*, 1909–1920.
11. Scheel, J., Pierre, P., Rickard, J.E., Diamantopoulos, G.S., Valetti, C., van der Goot, F.G., Haner, M., Aebi, U., and Kreis,

T.E. (1999). Purification and analysis of authentic CLIP-170 and recombinant fragments. J. Biol. Chem. *274*, 25883–25889.

12. Perez, F., Diamantopoulos, G.S., Stalder, R., and Kreis, T.E. (1999). CLIP-170 highlights growing microtubule ends in vivo. Cell *96*, 517–527.
13. Diamantopoulos, G.S., Perez, F., Goodson, H.V., Batelier, G., Melki, R., Kreis, T.E., and Rickard, J.E. (1999). Dynamic localization of CLIP-170 to microtubule plus ends is coupled to microtubule assembly. J. Cell Biol. *144*, 99–112.
14. Brunner, D., and Nurse, P. (2000). CLIP170-like tip1p spatially organizes microtubular dynamics in fission yeast. Cell *102*, 695–704.
15. Komarova, Y.A., Akhmanova, Y.A., Kojima, S., Galjart, N., and Borisy, G.G. (2002). Cytoplasmic linker proteins promote microtubule rescue in vivo. J. Cell Biol. *159*, 589–599.
16. Busch, K.E., Hayles, J., Nurse, P., and Brunner, D. (2004). Tea2p kinesin is involved in spatial microtubule organization by transporting tip1p on microtubules. Dev. Cell *6*, 831–843.
17. Carvalho, P., Gupta, M.L., Jr., Hoyt, M.A., and Pellman, D. (2004). Cell cycle control of kinesin-mediated transport of Bik1 (CLIP-170) regulates microtubule stability and dynein activation. Dev. Cell *6*, 815–829.
18. Rickard, J.E., and Kreis, T.E. (1991). Binding of pp170 to microtubules is regulated by phosphorylation. J. Biol. Chem. *266*, 17597–17605.
19. Choi, J.H., Bertram, P.G., Drenan, R., Carvalho, J., Zhou, H.H., and Zheng, X.F. (2002). The FKBP12-rapamycin-associated protein (FRAP) is a CLIP-170 kinase. EMBO Rep. *3*, 988–994.
20. Busch, K.E., and Brunner, D. (2004). The microtubule plus end-tracking proteins mal3p and tip1p cooperate for cell-end targeting of interphase microtubules. Curr. Biol. *14*, 548–559.
21. Walker, R.A., O'Brien, E.T., Pryer, N.K., Soboeiro, M.F., Voter, W.A., Erickson, H.P., and Salmon, E.D. (1988). Dynamic instability of individual microtubules analyzed by video light microscopy: Rate constants and transition frequencies. J. Cell Biol. *107*, 1437–1448.
22. Gildersleeve, R.F., Cross, A.R., Cullen, K.E., Fagen, A.P., and Williams, R.C. (1992). Microtubules grow and shorten at intrinsically variable rates. J. Biol. Chem. *267*, 7995–8006.
23. Chrétien, D., Fuller, S.D., and Karsenti, E. (1995). Structure of growing microtubule ends: Two-dimensional sheets close into tubes at variable rates. J. Cell Biol. *129*, 1311–1328.
24. Drechsel, D.N., Hyman, A.A., Cobb, M.H., and Kirschner, M.W. (1992). Modulation of the dynamic instability of tubulin assembly by the microtubule-associated protein tau. Mol. Biol. Cell *3*, 1141–1154.
25. Gaskin, F., and Cantor, C.R. (1974). Turbidimetric studies of the in vitro assembly and disassembly of Porcine neurotubules. J. Mol. Biol. *89*, 737–758.
26. Kirschner, M.W., Williams, R.C., Weingarten, M., and Gerhart, J.C. (1974). Microtubules from mammalian brain: Some properties of their depolymerization products and a proposed mechanism of assembly and disassembly. Proc. Natl. Acad. Sci. USA *71*, 1159–1163.
27. Howard, W.D., and Timasheff, S.N. (1986). GDP state of tubulin: Stabilization of double rings. Biochemistry *25*, 8292–8300.
28. Melki, R., Carlier, M.F., Pantaloni, D., and Timasheff, S.N. (1989). Cold depolymerisation of microtubule to double rings: Geometric stabilization of assemblies. Biochemistry *28*, 9143–9152.
29. Nogales, E., Wang, H.W., and Niederstrasser, H. (2003). Tubulin rings: Which way do they curve? Curr. Opin. Struct. Biol. *13*, 256–261.
30. Mandelkow, E.M., Mandelkow, E., and Milligan, R.A. (1991). Microtubule dynamics and microtubule caps: A time-resolved cryo-electron microscopy study. J. Cell Biol. *114*, 977–991.
31. Tran, P.T., Joshi, P., and Salmon, E.D. (1997). How tubulin subunits are lost from the shortening ends of microtubules. J. Struct. Biol. *118*, 107–118.
32. Müller-Reichert, T., Chrétien, D., Severin, F., and Hyman, A.A. (1998). Structural changes at microtubule ends accompanying GTP hydrolysis: Information from a slowly hydrolyzable analogue of GTP, guanylyl(alpha,beta)methylenediphosphonate. Proc. Natl. Acad. Sci. USA *95*, 3661–3666.
33. Arnal, I., Karsenti, E., and Hyman, A.A. (2000). Structural transitions at microtubule ends correlate with their dynamic properties in Xenopus egg extracts. J. Cell Biol. *149*, 767–774.
34. Spann, U., Renner, W., Mandelkow, E.M., Bordas, J., and Mandelkow, E. (1987). Tubulin oligomers and microtubule assembly studied by time-resolved X-ray scattering: Separation of prenucleation and nucleation events. Biochemistry *26*, 1123–1132.
35. Andersen, S.S., and Karsenti, E. (1997). XMAP310: A Xenopus rescue-promoting factor localized to the mitotic spindle. J. Cell Biol. *139*, 975–983.
36. Caudron, N., Arnal, I., Buhler, E., Job, D., and Valiron, O. (2002). Microtubule nucleation from stable tubulin oligomers. J. Biol. Chem. *277*, 50973–50979.
37. Job, D., Valiron, O., and Oakley, B. (2003). Microtubule nucleation. Curr. Opin. Cell Biol. *15*, 111–117.
38. Vasquez, R.J., Gard, D.L., and Cassimeris, L. (1994). XMAP from Xenopus eggs promotes rapid plus end assembly of microtubules and rapid miotubule polymer turner. J. Cell Biol. *127*, 985–993.
39. Cassimeris, L., Gard, D., Tran, P.T., and Erickson, H.P. (2001). XMAP215 is a long thin molecule that does not increase microtubule stiffness. J. Cell Sci. *114*, 3025–3033.
40. Erickson, H.P. (1974). Assembly of microtubules from preformed, ring-shaped protofilaments and 6-S tubulin. J. Supramol. Struct. *2*, 393–411.
41. Kirschner, M.W., Honig, L.S., and Williams, R.C. (1975). Quantitative electron microscopy of microtubule assembly in vitro. J. Mol. Biol. *99*, 263–276.
42. Tirnauer, J.S., Grego, S., Salmon, E.D., and Mitchison, T.J. (2002). EB1-microtubule interactions in Xenopus egg extracts: Role of EB1 in microtubule stabilization and mechanisms of targeting to microtubules. Mol. Biol. Cell *13*, 3614–3626.
43. Ashford, A., Andersen, S.S.L., and Hyman, A.A. (1998). Preparation of tubulin from bovine brain. In Cell Biology: A Laboratory Handbook. 2nd edition. Vol. 2. Julio E. Cells, ed. (Academic Press, Inc., Orlando, FL.), pp. 205–212.
44. Bornens, M., Paintrand, M., Berges, J., Marty, M.C., and Karsenti, E. (1987). Structural and chemical characterization of isolated centrosomes. Cell Motil. Cytoskeleton *8*, 238–249.
45. Chrétien, D., Buendia, B., Fuller, S.D., and Karsenti, E. (1997). Reconstruction of the centrosome cycle from cryoelectron micrographs. J. Struct. Biol. *120*, 117–133.
46. Dubochet, J., Adrian, M., Lepault, J., and McDowall, A. (1985). Cryo-electron microscopy of vitrified biological specimens. Trends Biochem. Sci. *10*, 143–146.